ISBN: 978-3-95450-233-2 ISSN: 2673-5504 doi:10.18429/JACoW-SRF2021-FROFDV03

INVESTIGATING THE ANOMALOUS FREQUENCY VARIATIONS NEAR T_C OF Nb SRF CAVITIES

D. Bafia*, M. Checchin, A. Grassellino, A.S. Romanenko
Fermi National Accelerator Laboratory, Batavia, IL, USA
J. F. Zasadzinski, Illinois Institute of Technology, Chicago, IL, USA

Abstract

We report recent studies on the anomalous frequency variations of 1.3 GHz Nb SRF cavities near the transition temperature T_c and use them to investigate the underlying physics of state-of-the-art surface treatments. One such feature, a dip in frequency, correlates directly with the quality factor at 16 MV/m and the anti-Q slope that arise in cavities with dilute concentrations of N interstitial in the RF layer achieved *via* N-doping and mid temperature baking. For N interstitial, we find that the dip magnitude and T_c follow exponential relationships with the electronic mean free path. We present the first observation of the frequency dip near T_c in a cavity baked at 200 °C *in-situ* for 11 hours, which is concurrent with the anti-Q slope, and may be driven by oxygen diffused from the native oxide, thus suggesting the possibility of "O-doping." We also investigate the conductivities of two cavities that display different resonant frequency behaviors near T_c and suggest that the anti-Q slope and frequency dip phenomena may occur in the presence of interstitial N or possibly O that inhibit the formation of proximity coupled Nb nano-hydrides.

INTRODUCTION

Most niobium superconducting radio-frequency (SRF) cavity research uses the quality factor Q_0 and thus the surface resistance R_s as a function of the accelerating gradient E_{acc} to gain insight on the microscopic mechanisms that enable the unprecedented performance of these resonators after undergoing various surface engineering treatments. However, there are far fewer studies on the resonant frequency f_0 behavior of cavities as a function of temperature, which yields valuable information on the surface reactance X_s and thus the superconducting carriers.

Recent work has shown that this frequency response holds a wealth of information. In particular, there exist features in the resonant frequency near the superconducting transition temperature T_c in bulk niobium SRF cavities that vary with surface processing and correlate well with cavity performance [1, 2]. This work shows that N-doped cavities, which exhibit high Q_0 and the anti-Q slope [3], a counterintuitive increase in Q_0 with E_{acc} that is suspected of having origins in non-equilibrium superconductivity [4] but has eluded full understanding, always produce a prominent dip in the resonant frequency just below the critical transition temperature. On the other hand, electropolished cavities [5], which are known to contain proximity coupled niobium nano-hydrides that drive high field Q-slope (HFQS) [6], often exhibit a sharp transition of the resonant frequency from the superconducting to the normal conducting regime, dubbed the standard feature. In addition, *in-situ* low temperature baked (LTB) cavities [5], which have historically achieved high quench fields, moderately high quality factors, and have been shown to mitigate HFQS by diffused oxygen preventing the precipitation of Nb nano-hydrides [7, 8], yield the foot feature in the frequency response near T_c, which describes a plateau of the resonant frequency just before going normal conducting. Such correlations between RF performance and frequency behavior stimulates continuing studies on the mechanisms at play as a full understanding would likely guide the development of new surface engineering protocols that further improve the performance of SRF cavities.

In this contribution, we investigate the frequency response near T_c of niobium SRF cavities subjected to state-of-the-art surface processing techniques (N-doping, mid-T baking, low temperature baking) and correlate with RF performance. We show that both nitrogen doped and mid-T baked cavities, which show high Q_0 and anti-Q slope, exhibit a prominent dip in the resonant frequency just before superconducting transition which is shown to scale with the measured quality factor at 16 MV/m. We find that the T_c and magnitude of the dip follow exponential relationships with the extracted electronic mean free path. Moreover, we show that *in-situ* low temperature baking brings about the anti-Q slope and dip phenomena *in the absence of nitrogen* and suggest that the behaviors may be driven by oxygen diffused from the native oxide, bringing about the concept of "oxygen doping." Lastly, to investigate possible differences in superconducting properties, we calculate and fit the complex AC superconducting conductivity of two cavities that exhibit different frequency features near T_c and find that the frequency dip and anti-Q slope occur when the average superconducting gap value is large and the inelastic scattering parameter is at a minimum, suggesting that these behaviors may be inherent to niobium that is void of proximity coupled inclusions.

EXPERIMENTAL

We performed our studies on TESLA-shaped 1.3 GHz bulk niobium single-cell SRF cavities that underwent a bulk removal from the inner RF surface *via* EP followed by an 800 °C degassing step and an additional 30 µm EP removal from the inner RF surface. Cavities were then treated with different state-of-the-art surface treatments, including nitrogen doping [3] and *in-situ* low temperature baking [5]. Note that nitrogen doping is usually referred to as "x/y + z µm

* dbafia@fnal.gov

ISBN: 978-3-95450-233-2 ISSN: 2673-5504 doi:10.18429/JACoW-SRF2021-FROFDV03

EP" doping, where x is the duration of the annealing stage in nitrogen in minutes, y is the duration of the vacuum annealing stage in minutes, and z is the thickness of material removed from the inner RF surface *via* electropolishing after the furnace treatment.

We measured the RF performance of cavities using the methods laid out in [9]. Cavities were equipped with Helmholtz coils and resistance temperature detectors (RTDs) and flux gates at the equator. We used the typical fast cool down protocol in zero compensated field to minimize the effect of trapped magnetic flux. To decompose the obtained Q_0 vs E_{acc} into the temperature dependent BCS resistance R_{BCS} and material dependent residual resistance R_{res}, we performed the RF tests at both 2 K and <1.5 K and used the methods laid out in [10].

After RF tests were completed, we measured the cavity resonant frequency as a function of temperature. We used a vector network analyzer (VNA) to measure the S21 signal while slowly increasing the dewar temperature. To carry this out, we applied low power to heaters located at the bottom of the dewar while it was open to atmosphere. This method allowed for a slow warming rate of <0.1 K/min, ensuring full thermalization of the cavity, as confirmed by the RTDs. All data was corrected to filter out contributions from pressure variations. We choose to present frequency data as a frequency shift relative to the normal conducting value ($f_{0,NC}$), such that $\Delta f_0(T) = f_0(T) - f_{0,NC}$.

EFFECT OF NITROGEN CONCENTRATION ON NEAR T_c FREQUENCY FEATURES

In this section, we delineate the role of nitrogen concentration in the frequency dip near T_c of bulk niobium SRF cavities. We subjected a single cavity, TE1RI003, to 3/60 nitrogen doping and tested it after sequentially removing the inner RF with electropolishing. This gradually decreased the concentration of nitrogen present within the RF layer. The RF and $\Delta f_0(T)$ measurements obtained after each step are shown in Fig. 1.

To obtain some measure of the nitrogen concentration after each step in Fig. 1, we extracted an effective mean free path ℓ for each data set by converting to a shift in the magnetic penetration depth *via* Slater's theorem [11] and fitting with the modified Halbritter routine [12]. The extracted ℓ values are shown in the legend in Fig. 1.

After the initial test post 3/60 + 10 µm EP N-doping, the cavity exhibited high Q_0 at 3E10 at mid field, the characteristic anti-Q slope, and a prominent dip in the resonant frequency with magnitude Δf_{dip} = 1.3 kHz just before T_c at 9.20 K. Upon decreasing the concentration of nitrogen (or increasing the effective ℓ), we observed that the Q_0, degree of anti-Q slope, and Δf_{dip} decreased while T_c increased. After a total removal of 30 µm from the inner, coinciding with ℓ = 500 nm, the cavity exhibited typical HFQS behavior with an onset at 25 MV/m, indicating the existence of proximity coupled nano-hydrides within the RF layer [6] and that any

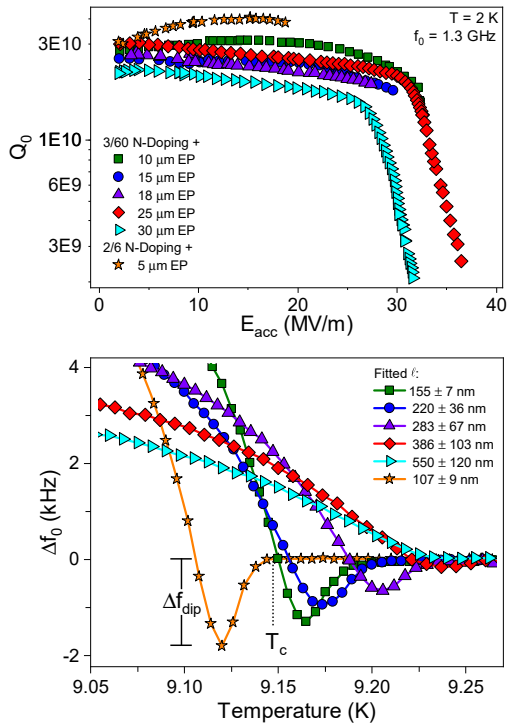

Figure 1: Q_0 vs E_{acc} and $\Delta f_0(T)$ measurements of cavity TE1RI003 subjected to a single nitrogen doping surface treatment followed by sequential removal from the inner RF surface *via* EP. The legend in the lower plot shows the fitted effective mean free path for each step of removal.

benefit of nitrogen doping had been lost. Furthermore, the dip in resonant frequency was replaced by the "standard" feature, showing a sharp transition from the superconducting to the normal conducting regime. The cavity was then reset with EP and retreated with the 2/6 + 5 µm EP nitrogen doping surface treatment, which produced the shortest mean free path (107 nm), largest Q_0, largest degree of anti-Q slope, lowest T_c, and the largest Δf_{dip} in this study.

Figure 2 plots the quality factor measured at a field of 16 MV/m against the measured dip magnitude of many 1.3 GHz cavities subjected to either variants of nitrogen doping or mid-T baking, the latter which comes from Posen *et al.* [13]. Note that mid-T baking has been found to introduce nitrogen into the RF layer, thus possibly driving the doping effect in cavities subjected to this surface treatment. The two sets of data seem to find follow a linear trend and suggests that the quality factor and the dip phenomenon are tied to the same interface properties.

In Fig. 3, we plot the measured T_c and Δf_{dip} (as defined in Fig. 1) against the average electronic mean free path. The dip magnitude decreases almost exponentially with increasing ℓ or decreasing nitrogen concentration. The dependence of T_c is also well modelled by an exponential relationship with the MFP and varies about 270 mK for the given data. These values agree well with previous studies on the effect of nitrogen on the T_c of niobium [14] and may be due to a reduction of the anisotropy of the superconducting gap due

ISBN: 978-3-95450-233-2 ISSN: 2673-5504 doi:10.18429/JACoW-SRF2021-FROFDV03

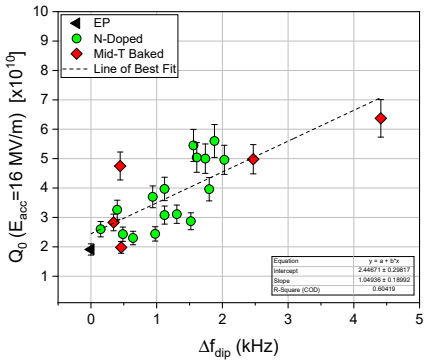

Figure 2: Q_0 measured at a field of 16 MV/m plotted against the dip magnitude Δf_{dip} of nitrogen doped and mid-T baked cavities. Shown also for reference is data on an EP cavity, which shows no frequency dip feature. Mid-T bake data comes from [13].

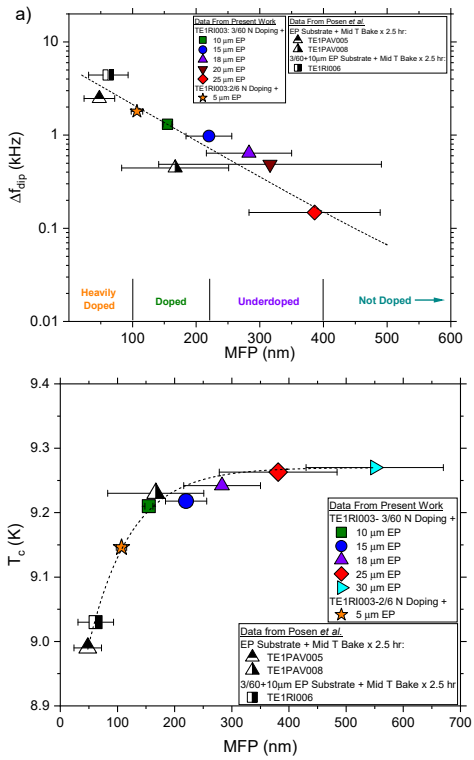

Figure 3: Dip magnitude and transition temperature (defined in Fig. 1) plotted against the fitted effective mean free path of nitrogen doped and mid-T baked cavities. Mid-T bake data comes from [13].

to scattering [15]. We also show a proposed nitrogen doping level assessment scheme, which may be used to categorize different levels of nitrogen doping.

To summarize this section, we show that the concentration of nitrogen in the RF layer determines the Q_0, anti-Q slope, T_c, and Δf_{dip} in niobium SRF cavities. We also suggest that the problem of identifying the origins of ultra-high Q_0 and/or anti-Q slope may reduce to the problem of understanding the mechanisms responsible for the dip phenomenon.

EFFECT OF LOW TEMPERATURE BAKING ON NEAR T_c FREQUENCY FEATURES

Previous work has shown that the *in-situ* low temperature bake often brings about a foot feature in the resonant frequency just before T_c, marked a plateau in the frequency before going normal conducting [2]; here we study the evolution of this feature with increasing *in-situ* bake durations. A single cavity, TE1AES019, was fully assembled, evacuated, and baked with a 90 °C *in-situ* bake for 384 hour to eliminate high field Q slope [16]. It was then subjected to sequential rounds of baking at 200 °C and tested after each step. The results are shown in Fig. 4. We note that the cavity maintained vacuum throughout the course of the study, preventing the growth of the native oxide layer after baking.

From Fig. 4, after the first round of baking (+200 °C for 1 hour), we observed the expected behaviors of *in-situ* LTB cavities: a higher quench field, a larger BCS resistance and non-monotonic dependence on the field, and a small but present foot feature in the resonant frequency just before T_c. However, the results after the next round of 200 °C baking, for an integrated bake duration of 11 hours, were surprising. The Q_0 vs E_{acc} curve exhibited an anti-Q slope behavior, as confirmed by the BCS resistance. Furthermore, the foot feature in the frequency near T_c was replaced by a prominent dip with $\Delta f_{\text{dip}} \approx 0.4$ kHz. However, the T_c remained constant at ~9.27 K.

As such behaviors are characteristic of cavities processed with surface treatments that introduce uniform and dilute concentrations of nitrogen into the RF layer (nitrogen doping [3] and mid-temperature baking [13]), we originally suspected that the 200 °C low temperature *in-situ* baking treatment was somehow introducing nitrogen into the niobium lattice.

To determine what might be driving this doping effect after *in-situ* low temperature baking at 200 °C for 11 hours, we performed time-of-flight secondary ion mass spectroscopy (TOF-SIMS) on an as-received electropolished cavity cutout after baking it *in-situ* at 205 °C for 19 hours without ever breaking vacuum, thus effectively recreating the surface treatment used on the cavity. We used the same IONTOF TOF-SIMS system described in [7] with a liquid Bi^+ ion beam to perform secondary ion measurements while sputtering with a Cs^+ ion gun with energy 1 keV to obtain impurity profiles with depth. The results are shown in Fig. 5.

Interestingly, we found that the NbN^-/Nb^- ion signal, which we interpret as a measure of the level of nitrogen, remained at the background level just below the oxide even after the 205 °C bake for 11 hours. This is further reinforced when comparing the NbN^-/Nb^- ion signals to that measured on an as received 2/6 N-doped cavity cutout, showing over an order of magnitude difference. As such, there was likely no nitrogen present in the RF layer after the 200 °C × 11 hour *in-situ* LTB, and the doping behaviors observed in Fig. 4 may have been driven by another mechanism.

ISBN: 978-3-95450-233-2 ISSN: 2673-5504 doi:10.18429/JACoW-SRF2021-FROFDV03

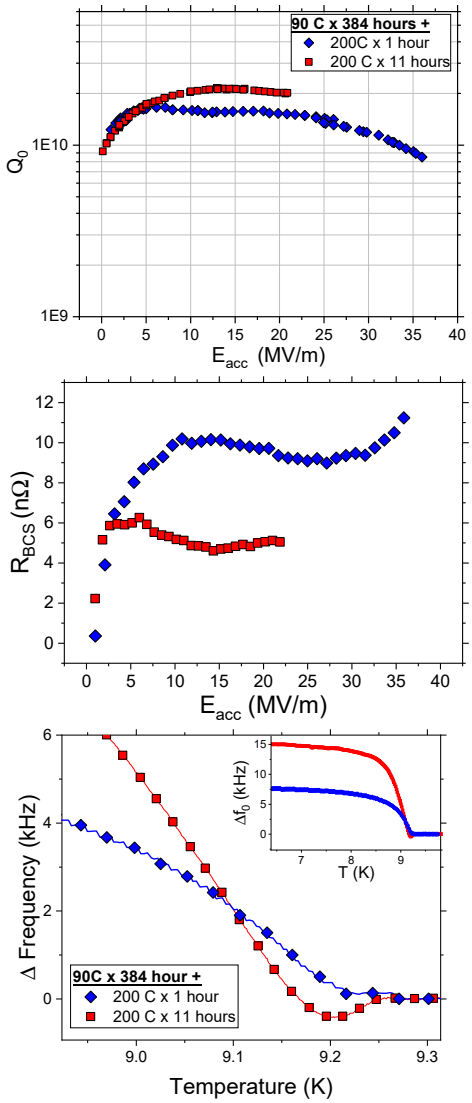

Figure 4: Q_0 vs E_{acc} at 2 K, BCS resistance at 2 K, and $\Delta f_0(T)$ curves of TE1AES019 after sequential rounds of low temperature *in-situ* baking. The inset in the lowest plot shows the frequency response over a larger range of temperatures. The durations shown in the legends represent the integrated bake times.

One possible driver for the doping behavior observed in Fig. 4 after 200 °C × 11 hour *in-situ* LTB may stem from the diffusion of oxygen from the native oxide toward the niobium bulk. It has been previously shown on niobium SRF cavity cutouts that low temperature baking causes oxygen to diffuse from the oxide according to Fick's law [7, 8, 17]. Indeed, the lower plot in Fig. 5 shows that the 75/120 °C *in-situ* bake only diffuses oxygen to a depth of about 100 nm from the RF surface and shows a large gradient in the measured O^-/Nb^- ion signal over the RF layer. Such cavities do not exhibit the anti-Q slope phenomenon nor the frequency dip feature [2, 18, 19]. However, the results of the EP cavity cutout after *in-situ* LTB at 200 °C for 19 hours show that the oxygen signal extends to roughly 1000 nm and produces a more uniform concentration within the RF layer. While more

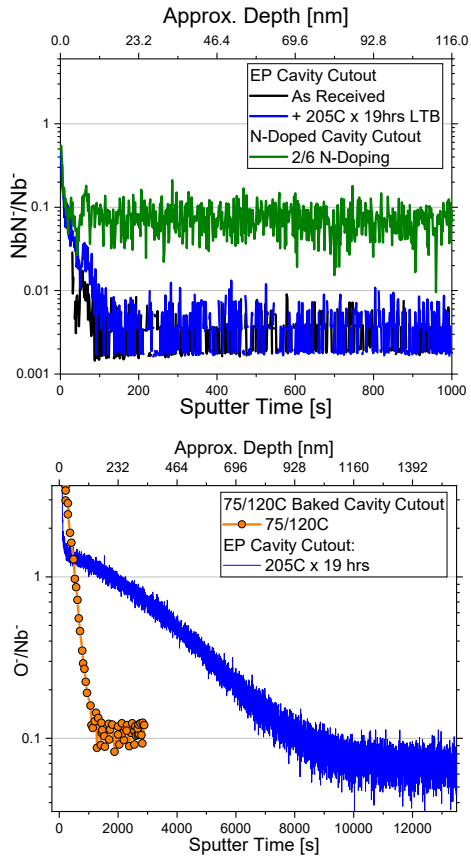

Figure 5: TOF-SIMS acquired depth profiles on an as-received EP cavity cutout measured before and after *in-situ* baking at 205 °C for 19 hours. Shown also are depth profiles taken on an as received 2/6 N-doped cavity cutout and a 75/120 °C baked cavity cutout. All signals are normalized point-by-point to the Nb^- ion signal. Note that the RF layer extends ~100 nm from the surface.

studies are required to pinpoint the exact mechanism, these results suggest that the uniform concentration of oxygen present within the RF layer may be responsible for driving the anti-Q slope and dip phenomena observed in Fig. 4 after *in-situ* low temperature baking, thus bringing about the concept of "oxygen doping". This is in agreement with a recent and independent study that has suggested the role of oxygen in the anti-Q slope phenomenon in the absence of nitrogen [20]

With the possibility of oxygen driving the doping behavior of cavities after *in-situ* low temperature baking, this begs the question: how does "oxygen doping" compare with nitrogen doping? Figure 6 makes such a comparison and plots the results from TE1AES019 after 90 °C × 384 hours + 200 °C × 11 hours *in-situ* low temperature baking, which we call "oxygen doped" and TE1RI003 after 3/60 + 10 µm EP N-doping from Fig. 1. We find that both treatments produce an almost identical behavior in the BCS resistance with field, showing that it decreases from 6 nΩ to about 5 nΩ.

ISBN: 978-3-95450-233-2 ISSN: 2673-5504 doi:10.18429/JACoW-SRF2021-FROFDV03

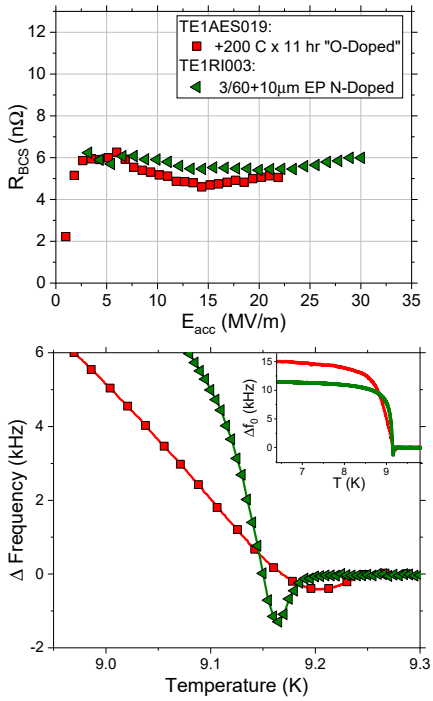

Figure 6: A comparison of the BCS resistance at 2 K and frequency response near T_c of cavity TE1AES019 after 90 °C × 384 hours + 200 °C × 11 hours *in-situ* low temperature baking from Fig. 4 and TE1RI003 after 3/60 + 10 µm EP N-doping from Fig. 1.

While the BCS resistance behavior is nearly identical, the frequency behavior differs substantially, suggesting a dependence on the dopant species. The "oxygen doped" cavity follows an almost linear decrease in frequency with temperature above ~8.7 K that is not present in the N-doped cavity. We also see that the transition temperature of the nitrogen doped cavity is lower than what is achieved post "oxygen doping". This is surprising as oxygen has been shown to more strongly suppress the T_c of niobium than nitrogen for a given concentration [14]. This might be indicating that, when compared to nitrogen impurities, a lower concentration of oxygen in the RF layer is required to bring about the decrease in the BCS resistance with field driven by non-equilibrium effects that results in the anti-Q slope. Further studies are needed to test this suspicion. We also find that the "oxygen doped" cavity exhibits a smaller Δf_{dip} but a wider full width half max. This latter observation could be suggesting the existence of a larger distribution of T_c, as suggested in AC magnetic susceptibility studies on high temperature superconductors [21], which may be indicating a greater level of inhomogeneity on the inner RF surface. Again, further studies are required to explore this possibility.

Reference [16] discusses further studies on the role of oxygen in the performance of niobium SRF cavities.

To conclude this section, we find that the role that oxygen plays in the performance of SRF cavities after *in-situ* low temperature baking for extended durations *may* be similar to that of nitrogen after nitrogen doping and suggest that uniform concentrations of oxygen in the RF layer may bring about the anti-Q slope and dip phenomena, thus introducing the concept of "oxygen doping. We also find that the frequency behavior near T_c gives further insight on superconducting properties and that it likely depends on dopant species.

IMPLICATIONS ON THE COMPLEX CONDUCTIVITY

While a full microscopic understanding of the frequency features near T_c has not yet been realized, we explored the conditions under which they occur by investigating the AC complex conductivity $\sigma(T) = \sigma_1(T) + i\sigma_2(T)$. Using the method laid out by Trunin [22], the AC complex conductivity may be extracted using surface impedance measurements $Z_s(T) = R_s(T) + iX_s(T)$ over the temperature range of interest *via*

$$\sigma = \sigma_1 + i\sigma_2 = \omega\mu_0\left(\frac{2R_sX_s}{(R_s^2+X_s^2)^2} + i\frac{X_s^2 - R_s^2}{(R_s^2+X_s^2)^2}\right), \quad (1)$$

where the surface resistance and reactance are defined by

$$R_s(T) = \frac{G}{Q_0(T)} \quad (2)$$

$$X_s(T) = -2G\frac{\Delta f_0(T)}{f_0} + X_n, \quad (3)$$

where $G = 270\,\Omega$ is the geometry factor of TESLA shaped cavities and X_n is the normal conducting reactance measured at ~10 K, which must consider anomalous skin effects [23]. Further details on the calculation of the complex conductivity from impedance measurements may be found in [2].

To gain further insights on quasi-particle and superconducting carrier dynamics that may give a better understanding of the underlying physics at play behind the anti-Q slope and the frequency dip, we measured σ of two niobium cavities that exhibited different RF behaviors and frequency features near T_c: i) an electropolished cavity (TE1RI003) ii) a 2/6 + 5 µm EP N-doped cavity (TE1PAV009).

Figure 7 summarizes the RF, BCS resistance, and frequency vs temperature results of TE1RI003 and TE1PAV009 and shows all of the otherwise expected behaviors. TE1PAV009 post nitrogen doping exhibited high Q_0 at mid field and anti-Q slope that was driven by the decrease in the BCS resistance with field. It also showed a prominent dip in resonant frequency just before the normal conducting transition at 9.04 K, which gives a MFP of ~70 nm by extrapolating from Fig. 3. TE1RI003, on the other hand, exhibited HFQS beginning at ~25 MV/m, an increasing BCS resistance with field, and the "standard" frequency feature near T_c. The fitted MFP was 550 ± 120 nm.

To measure the surface impedance over the entire temperature range of interest for the two cavities, we used the methods laid out in [24]; the results are shown in Fig. 8. Note that the dip in frequency becomes a peak in reactance due to the change of signs in Eq. (3).

ISBN: 978-3-95450-233-2 ISSN: 2673-5504 doi:10.18429/JACoW-SRF2021-FROFDV03

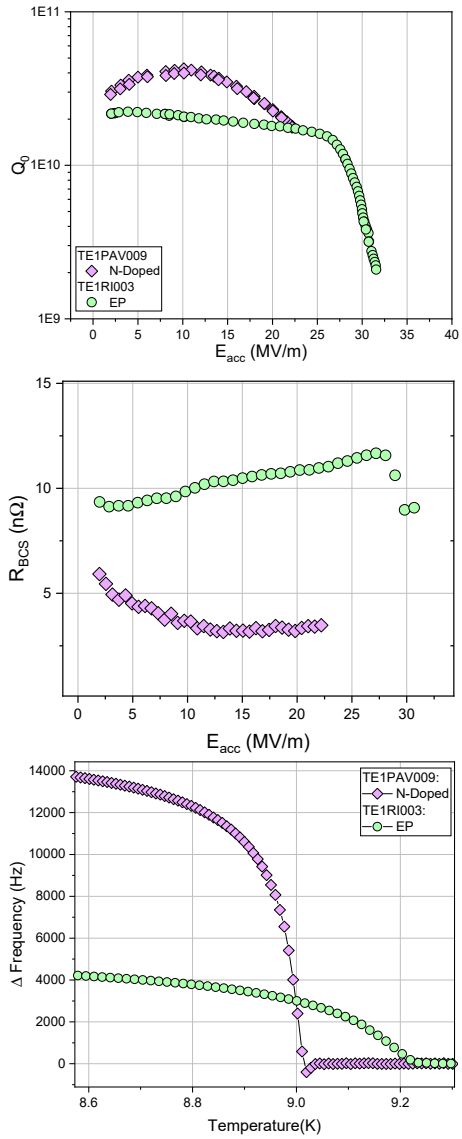

Figure 7: Measured Q_0 vs E_{acc} at $T = 2$ K, BCS resistance at 2 K, and frequency response as a function of temperature of TE1PAV009 after 2/6 + 5 µm EP nitrogen doping and TE1RI003 after electropolishing.

As a check of our method, we calculated the penetration depth at 0 K directly from our measured surface reactance *via*

$$X_{s,0} = \omega\mu_0\lambda_{0,\mathrm{exp}} \tag{4}$$

and compared it to the value obtained using Pippard theory

$$\lambda_0 = \lambda_L\sqrt{1+\frac{\xi_0}{\ell}}. \tag{5}$$

Table 1 shows excellent agreement between the two methods for both cavities.

To calculate the AC conductivity, we used the data shown in Fig. 8 in Eq. (1); the results are shown in Fig. 9. Error bars for TE1PAV009 (TE1RI003) are dominated by uncertainty in the measurement (error in fitted ℓ value). For both of the studied cavities, we observe the existence of the so-called

Table 1: Comparison of Experimentally and Theoretically Calculated Penetration Depths

$\lambda_{0,\,\mathrm{exp}}$ [nm]	λ_0 [nm]
36 ± 8	40
54 ± 2	48

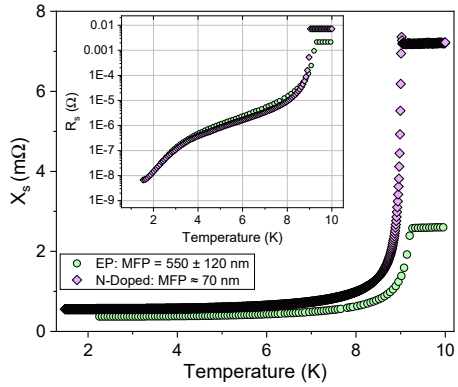

Figure 8: Measured surface reactance and surface resistance with temperature of TE1PAV009 post 2/6 + 5 µm EP N-doping and TE1RI003 after electropolishing.

coherence peak near 0.9 T/T_c but with differing amplitudes. The coherence peak arises due to coherence factors in BCS theory [25] and is analogous to the Hebel-Schlichter peak in nuclear spin relaxation [26]. To the best of our knowledge, this is the first time the coherence peak has been reported in bulk niobium SRF cavities.

As a simple phenomenological model to fit our data, we used the Mattis-Bardeen model of the AC complex conductivity [27] with the Dynes inelastic scattering parameter Γ [28] built into the density of states, given as

$$\frac{\sigma_1}{\sigma_n} = \frac{2}{\hbar\omega}\int_{\Delta}^{\infty}\frac{[f(E)-f(E+\hbar\omega)]g(E,\Gamma)}{\sqrt{(E+i\Gamma)^2-\Delta^2}}dE + \frac{1}{\hbar\omega}\int_{\Delta-\hbar\omega}^{-\Delta}\frac{[1-2f(E+\hbar\omega)]g(E,\Gamma)}{\sqrt{(E+i\Gamma)^2-\Delta^2}}dE, \tag{6}$$

$$\frac{\sigma_2}{\sigma_n} = \frac{2}{\hbar\omega}\int_{\Delta-\hbar\omega,-\Delta}^{\Delta}\frac{[1-2f(E+\hbar\omega)]g(E,\Gamma)}{\sqrt{(\Delta^2-(E+i\Gamma)^2}}dE, \tag{7}$$

$$g(E,\Gamma) = \frac{(E+i\Gamma)((E+i\Gamma)+\hbar\omega)+\Delta^2}{\sqrt{((E+i\Gamma)+\hbar\omega)^2-\Delta^2}.}. \tag{8}$$

This model gives a measure of the level of pair-breaking present within the RF surface by introducing subgap quasiparticle states and reproduces some of the salient features in more rigorous theories at low values of Γ/Δ [29–31]. As shown in dashed and solid lines in Fig. 9, the model gives good fits with experimental data.

From the fits, we find that both σ_1/σ_n and σ_2/σ_n for TE1RI003 after EP are best modelled with an average superconducting gap of $\Delta_0 = 1.5$ meV and an inelastic scattering parameter $\Gamma/\Delta_0 = 0.025$. TE1PAV009 post N-doping is instead better fitted with a larger average super-

ISBN: 978-3-95450-233-2 ISSN: 2673-5504 doi:10.18429/JACoW-SRF2021-FROFDV03

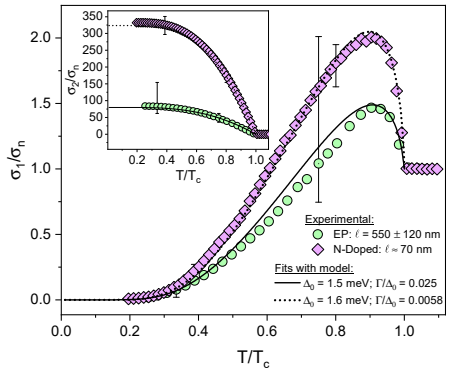

Figure 9: The real and imaginary parts of the AC complex conductivity normalized to the normal conducing value σ_n of TE1PAV009 after 2/6 + 5 µm EP nitrogen doping and TE1RI003 after electropolishing. Solid and dotted lines represent fits with Eqs. (6)-8.

conducting Δ_0 = 1.6 meV and a lower level of pair-breaking (Γ/Δ_0=0.0058).

These fitted values are consistent with point contact tunneling spectroscopy (PCTS) studies by Groll *et al.* on similarly treated cavity cutouts [32]. The N-doped samples in those studies showed slightly lower but more homogeneous Δ_0 values and lower levels of Γ/Δ_0 than those that came from EP cavities. This gives one possible cause for the difference in gap values obtained from the fits shown in Fig. 9; electropolished cavities contain localized defective regions that bring down the average superconducting gap. The lower level of pair-breaking observed in Fig. 9 for the N-doped cavity is likely due to the absence (or lower volume fraction) of proximity coupled nano-hydrides and magnetic moments within the interface. This is consistent with the fact that N-doped cavities do not exhibit the high field Q slope caused by the proximity breakdown of hydrides at high fields [3, 6] as nitrogen has been suggested to serve as an effective hydrogen trap [33], thus preventing hydride precipitation upon cool down to cryogenic temperatures.

While PCTS reports higher values of Γ/Δ_0 for both N-doped and EP samples than what is shown in fits with Fig. 9, this is likely due to differences in the probing depth between the two techniques. Since PCTS is more surface sensitive, it is likely that RF field measurements probe considerably deeper and sample regions with fewer pair-breaking mechanisms.

From the above, we suggest that the frequency dip and the anti-Q slope may occur when the average superconducting gap is large and the level of proximity coupling and magnetic moments within the RF layer are at a minimum.

The hypothesis that lower levels of inelastic scattering may enable the anti-Q slope and frequency dip may also explain the occurrence of these phenomena in cavities subjected to "oxygen doping" as oxygen has also been suggested to effectively capture free hydrogen [33], thus also diminishing or eliminating proximity coupled niobium nano-hydrides within the RF layer [7, 16]. The possibility that these phenomena exist independent of dopant species (but are manifested to slightly different extents depending on the dopant, as observed in Fig. 6) suggests that such behaviors may be inherent to niobium cavities that contain a minimal level of proximity coupled inclusions. Further studies are underway to test this hypothesis.

CONCLUSIONS

In this contribution, we have studied the performance of bulk niobium SRF cavities subjected to state-of-the-art surface treatments by studying their frequency response near the critical transition temperature. We found that dilute concentrations of nitrogen achieved *via* nitrogen doping or mid-T baking bring about the anti-Q slope and dip phenomena and that the nitrogen concentration determines the magnitude of the frequency dip and the critical transition temperature. Interestingly, we found that similar phenomena were obtained in a cavity subjected to 200 °C × 11 hours *in-situ* low temperature baking *in the absence of nitrogen*. This suggests that oxygen impurities may play a role in the performance of SRF cavities after low temperature baking that is similar to that of nitrogen after nitrogen doping, thus bringing about the concept of "oxygen doping". By investigating the frequency response of an oxygen doped cavity and a nitrogen doped cavity that both exhibited similar BCS resistance, we found evidence of inhomogeneity in the RF surface after oxygen doping, which may be key in understanding the underlying physics of this surface treatment. This observation also shows that that frequency response near T_c is a new lens through which the microscopic mechanisms responsible for improved performance may be studied. Lastly, by measuring and fitting the complex conductivities of EP and N-doped cavities, we showed that the anti-Q slope and dip phenomena are present when there exists a large average superconducting gap and a minimal level of proximity coupling within the RF layer. We suggest that this lower level of proximity coupling may be due to a lower volume fraction or elimination of proximity coupled nano-hydrides that are mitigated *via* interstitial nitrogen or perhaps even oxygen.

ACKNOWLEDGEMENTS

This manuscript has been authored by Fermi Research Alliance, LLC under Contract No. DE-AC02-07CH11359 with the U.S. Department of Energy, Office of Science, Office of High Energy Physics.

REFERENCES

[1] D. Bafia *et al.*, "New insights on nitrogen doping," in *Proc. SRF'19*, Dresden, Germany, Jun.-Jul. 2019. pp. 347-354. doi:10.18429/JACoW-SRF2019-TUFUA4

[2] D. Bafia, A. Grassellino, M. Checchin, J. F. Zasadzinski, and A. Romanenko, "The Anomalous Resonant Frequency Variation of Microwave Superconducting Niobium Cavities Near Tc," Mar. 2021. arXiv:2103.10601

[3] A. Grassellino *et al.*, "Nitrogen and argon doping of niobium for superconducting radio frequency cavities: a pathway to highly efficient accelerating structures," *Supercond. Sci.*

ISBN: 978-3-95450-233-2 ISSN: 2673-5504 doi:10.18429/JACoW-SRF2021-FROFDV03

Technol., vol. 26, p. 102001, Jul. 2013. doi:10.1088/0953-2048/26/10/102001

[4] M. Martinello *et al.*, "Field-enhanced superconductivity in high-frequency niobium accelerating cavities," *Phys. Rev. Lett.*, vol. 121, p. 224801, Nov. 2018. doi:10.1103/PhysRevLett.121.224801

[5] H. Padamsee, *RF Superconductivity: Volume II: Science, Technology, and Applications*, Wiley-VCH Verlag GmbH and Co., KGaA, Weinheim, 2009.

[6] A. Romanenko, F. Barkov, L. D. Cooley, and A. Grassellino, "Proximity breakdown of hydrides in superconducting niobium cavities," *Supercond. Sci. Technol.*, vol. 26,p. 035003, Jan. 2013. doi:10.1088/0953-2048/26/3/035003

[7] A. Romanenko, Y. Trenikhina, M. Martinello, D. Bafia, and A. Grassellino, "First direct imaging and profiling TOF-SIMS studies on cutouts from cavities prepared by state-of-the-art treatments," in *Proc. SRF'19*, Dresden, Germany, Jun.-Jul. 2019. pp. 866-870. doi:10.18429/JACoW-SRF2019-THP014

[8] A. Romanenko, A. Grassellino, and D. Bafia, "Oxygen role in the high field Q-slope/mild baking – revealed by TOF-SIMS + cavity surface engineering studies," presented at TTC'20, CERN, Geneva, Switzerland, Feb. 2020, unpublished.

[9] O. Melnychuk, A. Grassellino, and A. Romanenko, "Error analysis for intrinsic quality factor measurement in superconducting radio frequency resonators," *Rev. Sci. Instrum.*, vol. 85, p. 124705, Dec. 2014. doi:10.1063/1.4903868

[10] M. Martinello *et al.*, "Effect of interstitial impurities on the field dependent microwave surface resistance of niobium," *Appl. Phys. Lett*, vol. 109, p. 062601, Jul. 2016. doi:10.1063/1.4960801

[11] J. C. Slater, "Microwave electronics," *Rev. Mod. Phys.*, vol. 18, no. 4, p. 441, Oct. 1946. doi:10.1103/RevModPhys.18.441

[12] J. Halbritter, "FORTRAN-Program for the computation of the surface impedance of superconductors," Institut fur Experimentelle Kernphysik (IEKP), Report No. KFK-Extern 03/70-06, Jun. 1970.

[13] S. Posen *et al.*, "Ultralow surface resistance via vacuum heat treatment of superconducting radio-frequency cavities," *Phys. Rev. Appl.*, vol. 13, p. 014024, Jan. 2020. doi:10.1103/PhysRevApplied.13.014024

[14] W. DeSorbo, "Effect of dissolved gases on some superconducting properties of niobium," *Phys. Rev.*, vol. 132, p. 107, Oct. 1963. doi:10.1103/PhysRev.132.107

[15] D. Markowitz and L. P. Kadanoff, "Effect of impurities upon critical temperature of anisotropic superconductors," *Phys. Rev.*, vol. 131, p. 563, Mar. 1963. doi:10.1103/PhysRev.131.563

[16] D. Bafia, A. Grassellino, and A. Romanenko, "The role of oxygen concentration in enabling high gradients in niobium SRF cavities," presented at SRF'21, Jun.-Jul. 2021, paper THPTEV016, this conference.

[17] C. Benvenuti, S. Calatroni, and V. Ruzinov, "Diffusion of oxygen in niobium during bake-out," in *Proc. SRF'01*, CERN, Geneva, Switzerland, 2001. pp. 441-442.

[18] A. Grassellino *et al.*, "Accelerating fields up to 49 MV/m in TESLA-shape superconducting RF niobium cavities via 75C vacuum bake," Jun. 2019. arXiv:1806.09824

[19] D. Bafia *et al.*, "Gradients of 50 MV/m in TESLA shaped cavities via modified low temperature bake," in *Proc. SRF'19*, Dresden, Germany, Jun.-Jul. 2019. pp. 586-591. doi:10.18429/JACoW-SRF2019-TUP061

[20] E. Lechner *et al.*, "RF surface resistance tuning of superconducting niobium via thermal diffusion of native oxide," Jul. 2021. arXiv:2106.06647

[21] F. Gomory, "Characterization of high-temperature superconductors by AC susceptibility measurements," *Supercond. Sci. Technol.*, vol. 10, p. 523, Dec. 1997. doi:10.1088/0953-2048/10/8/001

[22] M. R. Trunin, A. A. Zhukov, and A. T. Sokolov, "Microwave impedance of Ba0.6K0.4BiO3 crystals: comparison with Nb," *Zh. Eksp. Teor. Fiz*, vol. 111, p. 696, Apr. 1997.

[23] G. E. H. Reuter and E. H. Sondheimer, "The theory of the anomalous skin effect in metals," *Proc. Roy. Soc. London Ser. A*, vol. 195, p. 336, Dec. 1948. doi:10.1098/rspa.1948.0123

[24] D. Bafia, "Exploring and Understanding the Limitations of Nb SRF Cavity Performance," Ph.D. thesis, Illinois Institute of Technology, Chicago, Illinois, 2020.

[25] J. Bardeen, L. N. Cooper, and J. R. Schrieffer, "Theory of superconductivity," *Phys. Rev.*, vol. 108, 5, p. 1175, Dec. 1957. doi:10.1103/PhysRev.108.1175

[26] L. C. Hebel and C. P. Slichter, "Nuclear spin relaxation in normal and superconducting aluminum," *Phys. Rev.*, vol. 113, p. 1504, Mar. 1959.

[27] D. C. Mattis and J. Bardeen, "Theory of the anomalous skin effect in normal and superconducting metals," *Phys. Rev.*, vol. 111,p. 412, Jul. 1958. doi:10.1103/PhysRev.111.412

[28] R. C. Dynes, V. Narayanamurti, and J. P. Garno, "Direct Measurement of Quasiparticle-Lifetime Broadening in a Strong-Coupled Superconductor," *Phys. Rev. Lett.*, vol. 41, p. 1509, Nov. 1978. doi:10.1103/PhysRevLett.41.1509

[29] T. Kubo, "Weak-field dissipative conductivity of a dirty superconductor with Dynes subgap states under a dc bias current up to the depairing current density," *Phys. Rev. Research*, vol. 2, p. 013302 Mar. 2020. doi:10.1103/PhysRevResearch.2.013302

[30] T. Kubo and A. Gurevich, "Field-dependent nonlinear surface resistance and its optimization by surface nanostructuring in superconductors," *Phys. Rev. B*, vol. 100, p. 064522, Aug. 2019. doi:10.1103/PhysRevB.100.064522

[31] F. Herman and R. Hlubina, "Electromagnetic properties of impure superconductors with pair-breaking processes," *Phys. Rev. B*, vol. 96, p. 014509, Jul. 2017. doi:10.1103/PhysRevB.96.014509

[32] N. R. Groll *et al.*, "Insight into bulk niobium superconducting RF cavities performances by tunneling spectroscopy," May. 2018. arXiv:1805.06359v1

[33] D. C. Ford, L. D. Cooley, and D. N. Seidman, "Suppression of hydride precipitates in niobium superconducting radio-frequency cavities," *Supercond. Sci. Technol.*, vol. 26, p. 105003, Aug. 2013. doi:10.1088/0953-2048/26/10/105003